Synergistic lubricating behaviors of graphene and MoS_2 dispersed in esterified bio-oil for steel/steel contact

Xu, Yufu; Peng, Yubin; Dearn, Karl D.; Zheng, Xiaojing; Yao, Lulu; Hu, Xianguo

DOI:
10.1016/j.wear.2015.09.011

Document Version
Peer reviewed version

Citation for published version (Harvard):
Xu, Y, Peng, Y, Dearn, KD, Zheng, X, Yao, L & Hu, X 2015, 'Synergistic lubricating behaviors of graphene and MoS_2 dispersed in esterified bio-oil for steel/steel contact', *Wear*, vol. 342-343, pp. 297-309. https://doi.org/10.1016/j.wear.2015.09.011

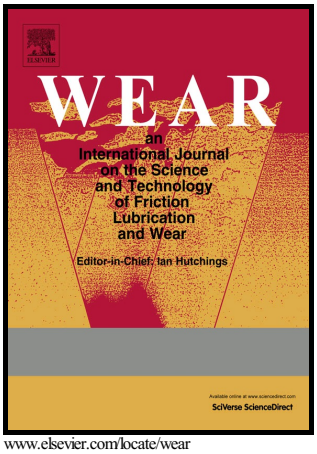

www.elsevier.com/locate/wear

Synergistic Lubricating Behaviors of Graphene and MoS_2 Dispersed in Esterified Bio-Oil for Steel/Steel Contact

Yufu Xu, Yubin Peng, Karl D. Dearn, Xiaojing Zheng, Lulu Yao, Xianguo Hu

PII: S0043-1648(15)00430-5
DOI: http://dx.doi.org/10.1016/j.wear.2015.09.011
Reference: WEA101509

To appear in: *Wear*

Received date: 28 July 2015
Accepted date: 22 September 2015

Cite this article as: Yufu Xu, Yubin Peng, Karl D. Dearn, Xiaojing Zheng, Lulu Yao and Xianguo Hu, Synergistic Lubricating Behaviors of Graphene and MoS Dispersed in Esterified Bio-Oil for Steel/Steel Contact, *Wear* http://dx.doi.org/10.1016/j.wear.2015.09.011

Synergistic Lubricating Behaviors of Graphene and MoS_2 Dispersed in Esterified Bio-Oil for Steel/Steel Contact

Yufu Xu[a *], Yubin Peng[a], Karl D Dearn[b], Xiaojing Zheng[c], Lulu Yao[d], Xianguo Hu[a]

a. Institute of Tribology, School of Mechanical and Automotive Engineering, Hefei University of Technology, Hefei 230009, China

b. School of Mechanical Engineering, University of Birmingham, Edgbaston, Birmingham, B152TT, United Kingdom

c. School of Arts and media, Hefei Normal University, Hefei 230601,China

d. School of Chemistry and Chemical Engineering, Hefei University of Technology, Hefei 230009, China

Abstract: Graphene and MoS_2 were dispersed in Esterified Bio-Oil (EBO) and evaluated as lubricants for steel/steel contact. The tribological behaviors of steel/steel pairs were investigated under lubrication of graphene/MoS_2 blends with different mass ratios, loads and rotating speeds. The micro-morphologies of the worn surfaces were observed by optical and Scanning Electron Microscopy (SEM). The components of the additives and chemical valences of the elements on the rubbed surfaces were analyzed using Raman and X-ray Photoelectron Spectroscopy (XPS). A synergistic lubricating effect for both graphene and MoS_2 with contents of 0.5 wt.% as additives dispersed in EBO was observed that reduced the friction coefficient and wear of the steel specimens under boundary lubrication regime conditions. This was ascribed to the formation of a thicker adsorbed tribo film containing graphene, MoS_2 and organics from the EBO. Graphene was shown to improve the retention of MoS_2 on the frictional surfaces and prevent oxidation during rubbing. MoS_2, on the other hand, prevented the graphene from being ground into small and defective platelets.

* Corresponding author. Tel/Fax.: +86-551-62901359.
E-mail address: xuyufu@hfut.edu.cn. (Y. F. Xu).

Key words: Steel; Boundary lubrication; Surface analysis; Sliding wear

1. Introduction

Multilayer materials such as molybdenum disulfide (MoS_2) have attracted lots of attention as both solid lubricants and additives in lubricating oils [1-6]. These studies have shown that MoS_2 may reduce frictional shearing by a mechanism of interlayer slippage, deformation, and exfoliation [7] . The friction-reducing properties of MoS_2 are easily removed during frictional rubbing , which can limit the antiwear effect. Recent research has reported that a single- or a few layers of graphene deposited on a steel surface, presents good adhesive properties and subsequently shows excellent wear resistance [8-12]. Collectively, the results of these studies suggest that graphene may be synergistically used with MoS_2 to enhance tribological performance. Currently, graphene/MoS_2 composites have been used as a photoresponse [13], electrochemical sensors [14], catalyst supports [15] and for lithium storage [16]. Very little research, however, has been done to study the lubricating properties of graphene/MoS_2 composites. These may be particularly effective where improvements to the lubricity of oils and lubricants are poor and require improvement. One such application is bio-oil.

The rise in the use of bio oil from fact pyrolysis is driven by a need to reduced fossil fuel usage and promising results in terms of emissions and engine performance [17-19]. The chemical composition of bio-oils are complex, containing carboxylic acids, aldehydes, alcohols, ketones, and phenols. Unfortunately, carboxylic acids are corrosive to metal surfaces, and this has resulted in the development of upgrading techniques for bio-oil. Separating acidic components from the bio-oil is extremely expensive, such that alternative, cheaper transfer technologies have been widely investigated. Through transferring acids to esters, esterified bio-oil (EBO) is prepared and has been

proved as a potential fuel product. However, the low heating value and high kinematic viscosity mean that EBO is more suitable as a base lubricating oil than a fuel used for combustion [20]. This therefore forms the basis of the need to study the friction and wear behaviors of base and additised esterified bio-oil with steel/steel frictional pairs for industrial applications. Xu *et al.* [21-24] have studied the lubricities and tribological behaviors of BO and EBO under different frictional conditions and have found that EBO has certain lubricating effects but requires improvement. In the present work, the tribological performance of graphene and MoS_2, dispersed separately and blended with EBO are reported, with a view as a potential lubricants for steel/steel contacts.

2. Experimental

2.1 Materials

The graphene was supplied by Hefei Vigon material technology Ltd. Co and the MoS_2 was purchased from the Shanghai chemical agents Ltd. Co. The size distribution of these two particles and their blends are shown in **Fig. 1**, indicating that both the graphene, MoS_2 and their blends comprise particles of about tens to several hundred micrometers in size. Figure 1 also serves to how that the blending process does not affect the structure or particle size.

EBO was prepared through catalytic esterification of crude bio-oil from *Spirulina* algae with ethanol at 50 ^{o}C for 5 hours over 5 wt.% KF/Al_2O_3 as a catalyst. The main components and their peak area contents, detected by GC-MS, were as follows: esters 17.23%, ketones 5.28%, N-containing organics 14.97%, aldehydes 5.62%, alkanes 1.9%, and furan 3.03%. More details of the upgrading process, oil components and physical properties of EBO can be found in [22].

Steel balls were used in the frictional tests with a diameter of 12.7 mm and were made from ASTM E52100 bearing steel with a hardness of 61–63 HRC.

2.2 Tribological tests

The graphene and MoS_2 were dispersed in the EBO with different mass ratios (0:1, 1:4, 2:3, 1:1, 3:2, 4:1, and 1:0) for 20 min with ultrasonic oscillation at room temperature (~26-28 ^{o}C),. The total content of additives in EBO was 0.5 wt.%. The dispersion stability of these additives was found to be acceptable with blends displaying stability for at least 240h after ultrasonic dispersion. Friction and wear tests for the pure EBO and EBO with additives were executed using a MQ-800 four-ball tribometer (Jinan Instrument Co., China) under a constant load of 300N and a rotational speed of 1000 rpm (0.383 m/s). Four selected EBO samples were tested under different loads of 100, 200, 300, 400, and 500N, and using different rotational speeds of 400, 550, 700, 850, 1000, 1150, 1300, and 1450 rpm, respectively. Every test was repeated three times. The friction coefficient was quarried automatically using the equipment's control system through the ratio of friction force to normal load, and its analysis accurate to ±0.01. The wear scar diameter (WSD) of the stationary specimens was the average values of the three lowers ones. The wear scar width (WSW) measured from the rotating sample. Both WSD and WSW were measured using an optical microscope with an accuracy of ±0.01 mm. A detailed schematic of the tribological tests is shown in **Fig. 2.** After frictional testing, the lubricants were filter and wear debris were separated by magnetic adsorption, the additives were then collected after being washed with acetone.

2.3 Characterization of materials and frictional surfaces

The size distributions of the graphene, MoS_2 and the blended particles, before and after testing were measured using an MS-2000 laser particle size analyzer (Malvern, UK). The microstructures, selected area electron diffraction (SAED) and powder X-ray diffraction (XRD) patterns of graphene

and MoS_2 particles were analyzed with an H800 transmission electron microscope (TEM, Hitachi, Japan) and a D/MAX2500V X-ray diffraction system (Rigaku, Japan),.

Raman spectroscopy of the additives before and after friction was analyzed on a LabRam HR Evolution Raman spectrometer (Horiba Jobin Yvon, France) with a 532 nm laser. The additives were processes operated to avoid sample damage.

An optical microscope and a JSM-6490LV (JEOL) SEM were used to analysis the micro-morphologies on the worn areas. An ESCALAB 250 (Thermo) XPS was used to analysis the chemical valences of the main elements on the worn surfaces. In addition to these techniques, a Talyor-Hobson-6 profilometer was employed to measure the worn surface roughness.

3. Results and discussion

3.1 Microstructures of graphene and MoS_2

The TEM image of graphene in **Fig. 3a** shows that the graphene nano-platelets are rippled and entangled with areas typically of a few square micrometers. Selected area electron diffraction (SAED) images in **Fig. 3a**(right) show diffraction rings that are well-defined and so the graphene nano-platelets have a crystalline structure and are well ordered. These results are confirmed by the XRD spectra in **Fig. 4a** by the strong (002) diffraction peak at ~26.4^o [25].

The typical layered structure of MoS_2 is clearly visible in **Fig. 3b**(left). The particle size is smaller than that from the laser particle analyzer. This may be due to aggregation of particles as was also observed by[26]. In addition, unambiguous diffraction rings in the SAED pattern of MoS_2 in **Fig. 3b** (right) confirm a crystalline structure, which is verified by the XRD pattern in **Fig. 4b**.

3.2 Influence of mass ratio of graphene and MoS_2 on tribological behavior

Fig. 5 shows the average friction coefficient and wear of steel balls lubricated by graphene and MoS_2 dispersed in EBO with different mass ratios. It can be seen that both graphene and MoS_2 as additives, can reduce the friction coefficient and wear of EBO. The strength of the effect of additives varies for different mass fractions, though there are the overlap of the error bars in some cases, and the similar frictional results have been reported by other researchers [27, 28]. Under the experimental conditions, MoS_2 was better at reducing friction, whereas graphene provided better wear resistance. When blended graphene and MoS_2,as a composite additive package have better friction reduction and antiwear properties than those of singular additive component. That is, there was a synergistic lubricating effect between graphene and MoS_2 dispersed in EBO, similar to that described in [29]. At the same time, with the increase in mass ratio of graphene to MoS_2, the EBO friction coefficient with additives, decreased to a point and then increased. The WSD and WSW of the worn surfaces show a similar pattern. Both the friction coefficient and wear was a minima when the mass ratio of graphene to MoS_2 was 3:2.

Fig. 6 shows the optical micrographs of the worn surfaces of rotating specimens under different lubricating conditions. The worn surface from the pure EBO has many obvious and wide furrows, indicating that pure EBO is ineffective at protecting the surfaces [22]. When graphene and MoS_2 was added, damage was reduced and the worn surfaces became smooth, suggesting an excellent lubricating effect of. The worn surface roughnesses are shown in **Fig. 7**. Once again, when the blend mass ratio of graphene to MoS_2 was 3:2, the worn surface was the smoothest. Based on the results shown in **Fig. 5,6 & 7**, a graphene to MoS_2 mass ratio of 3:2 was selected as the optimal additive package for further investigation of EBO tribological properties. As is reported [30, 31], loads and rotational speed can significantly alter the contact state of a frictional pair and affect lubricating mechanism

3.3 Influence of load and rotational speed on tribological behavior

Fig. 8 shows the influence of load on the friction coefficient and wear of the steel specimens lubricated by pure EBO, EBO with 0.5 wt.% graphene, EBO with 0.5 wt.% MoS_2, and EBO with 0.3 wt.% graphene and 0.2 wt.% MoS_2. Both the average friction coefficient, WSD and WSW of pure EBO increased gradually with load (from 100 to 500N). Higher loads can lead to smaller micro-intervals between the friction pairs [21], in the case of the experiments, there was less EBO at a molecular level that could be drawn into the frictional interface, increasing both friction coefficient and wear. For EBO with 0.5 wt.% graphene, the average friction coefficient and wear decreased gradually with load increasing. This may be because the graphene, as a solid lubricating film, was more easily squeezed and adsorbed on to the frictional surfaces at higher loads [32]. However, for EBO with 0.5 wt.% MoS_2 lubrication, increasing the load, reduced the average friction coefficient but rapidly increased it beyond 300N. The wear maintained a similar trend, being stable at first and then increasing rapidly. This effect may be the result of the thick MoS_2 layer being less likely to enter the frictional interface. If this is the case then it will also have been easier to be remove at higher loads, a phenomenon that is described in [33]. There was a large decrease in the average friction coefficient and wear of the EBO with 0.3 wt.% graphene and 0.2 wt.% MoS_2 lubrication, up to 300N. Beyond this load, both tribological effects either remain stable or increase. For the same load , the 3:2 EBO showed better lubricity than the three other lubricants. This confirms the synergistic lubricating effects between graphene and MoS_2 dispersed in EBO.

Fig. 9 shows the influence of rotational speed on the friction coefficient and wear of the steel test specimens lubricated by pure EBO, EBO with 0.5 wt.% graphene, EBO with 0.5 wt.% MoS_2, and EBO with 0.3 wt.% graphene and 0.2 wt.% MoS_2, respectively. It is noticeable from the Fig.9a

that, for pure EBO and EBO with 0.5 wt.% graphene lubrication, the average friction coefficient decreased gradually with the increase in rotational speed. This may be because of the higher frictional velocity, contributing to the decrease of the kinematic viscosity of EBO [34]. In case the EBO and graphene would have entered into the frictional interface to reduce the friction coefficient. At the higher rotational speeds, there is a rise in the friction coefficient at higher frictional speed when lubricated by EBO with 0.5 wt.% MoS_2. This is a result of the weak adsorption between the MoS_2 and the matrix, in this case the EBO . The 3:2 EBO had the lowest average friction coefficient which was constant, within experimental error for all frictional speeds, indicating that there was a complete and robust lubricating film on the tested surfaces[7].

From the Fig. 9b and c, it can be seen that the wear of steel specimens increased with the increase in rotational speed when lubricated by pure EBO. This can be explained by the fact that there was a longer sliding distance within the same test duration at higher rotational speeds. When graphene and MoS_2 were dispersed in EBO, the wear decreased significantly. Furthermore, EBO with 0.3 wt.% graphene and 0.2 wt.% MoS_2 had the lowest WSD and WSW, supporting the synergistic lubricating effects between graphene and MoS_2 again. From the Fig. 9c the EBO with additives, the increase of rotational speed, the WSW decreased at first and then increased. This suggests that an appropriate rotating speed at 850rpm (between 700 to 1000rpm) was helpful in the formation of a lubrication film. At low speeds, a tribo-reaction film was unable to form, but a high rotating speed might destroy the lubricating film and enlarge the wear. Combined the results of Fig. 8 and Fig. 9, the optimal frictional conditions for synergistic lubricating effects between graphene and MoS_2 were a load of 300N and a rotating speed of 850rpm. The synergistic lubricating mechanism for these conditions is further analyzed in the following section.

3.4 Friction and wear mechanism analysis

Fig. 10 shows the SEM images of the worn surfaces of steel/steel pairs lubricated by EBO and EBO with different additives. Furrows and adhesive pits on the worn surfaces lubricated by pure EBO can be clearly seen in Fig. 10a. These lubrication conditions also give the largest wear scar on the stationary specimen The main wear mechanism for pure EBO is ascribed to adhesive wear [35]. Some fine and dense furrows and few adhesive pits can be seen for the EBO with 0.5 wt.% graphene lubricated surfaces(Fig.10b). This suggests that graphene reduces wear. No clear wear debris was found on the worn surfaces, with a flash observed suggesting that the main wear mechanism was ploughing [36, 37]. Steel surfaces lubricated with EBO with 0.5 wt.% MoS_2 contain some spalling pits within worn furrows and heterogeneous wear scars (Fig.10c). The wear mechanism is likely to be a combination of ploughing and spalling [38]. The smoothest worn surface and the smallest wear scar are observed when lubricated by EBO with 0.3 wt.% graphene and 0.2 wt.% MoS_2 as additives (Fig.10d). Ploughing may once more be a factor in the wear of these surfaces [39]. The formation of a robust lubricating film, composed of adsorbed and tribo-reacted organics on the worn surfaces during the frictional process [40] may have minimized damage. This lubricating film was further studied by XPS in the following sections. The SEM micrographs, show surface damage that was in good agreement with the measured tribological behaviors.

To investigate the mutual influence of the graphene and MoS_2, the particle size distribution of the three additives after friction were measured and are shown in Fig. 11. Particle sizes are smaller than those before friction, shown in Fig.1. This suggests that the flake-additives were ground by the frictional process. However, when graphene and MoS_2 were used together, the morphology of the composite additive was maintained preventing wear to an extent.

Fig. 12 shows the Raman spectra of graphene, MoS_2 and their blends before and after friction. For graphene (Fig.12a), there is a typical peak at 1581cm^{-1}(G band) before friction, indicating a complete structure of sp^2 carbon in graphene [41]. However, a new peak at 1346cm^{-1} (D band) occurred after friction, which belongs to the sp^3 carbon group. This indicates that sp^2 carbon of graphene partially changed into sp^3 carbon due to friction. MoS_2 (Fig.12b) shows two typical peaks at 377cm^{-1} and 403cm^{-1} ascribed to $E_{2g}{}^1$ and A_{1g} modes of MoS_2 before friction. However, many new peaks at 196cm^{-1}, 283cm^{-1}, 482cm^{-1}, 564cm^{-1}, 662cm^{-1} emerged post rubbing, which are ascribed to MoO_3 or sulfate [42]. This suggested that MoS_2 is oxidized or reacts with the matrix or molecular in the EBO during the frictional process. When graphene and MoS_2 are used together (Fig.12c), both of the main peaks at 377cm^{-1}, 403cm^{-1} and 1581cm^{-1} of graphene and MoS_2 appeared before friction. After testing, no clear oxidation peaks of MoO_3 or sulfate can be observed. Their absence suggest that graphene helps to prevent MoS_2 from tribo-oxidation. Comparing this with the data in Fig.12a, the D band of graphene in Fig.12c shifted from 1346cm^{-1} to 1377cm^{-1}, and the ratio of I_D/I_G increased from 0.154 to 2.407 after friction. Both of these shifts are indicative of the formation of functional graphene due to a tribo-reaction between graphene and molecules in EBO. MoS_2 is likely to contribute to changing graphene into functional graphene and preventing defective graphene.

Combined with the results of particle size distribution and the Raman spectra, an illustration of the frictional process can be inferred, which is shown in Fig. 13. Graphene was effectively ground into small, defective particles when used on its own. MoS_2, as an individual additive is changed into MoO_3, sulfates and small particles during the frictional process. However, when graphene and MoS_2 are used together, the main frictional products are functional graphene and MoS_2.

XPS spectra of the typical elements on the worn surfaces of the rotational specimens are

shown in **Fig. 14.** The two C1s peaks located at binding energies of 284.8 eV and 288.7 eV, matched well with carbon or sp^3 C (C–C/C–H) and sp^2 C (C=C/C=O) [22], respectively. Both existed in these four samples. This indicated that the adsorbed film was composed of carbon or/and organics containing ester, which will have been derived from the graphene or/and EBO, and which played a protective role during the rubbing process. The largest areas of these two peaks(d) in the C1s suggests that graphene and MoS_2 blends dispersed in EBO contributed to forming the thickest adsorbed film containing graphene and organics. The highest ratio of $I_{sp}{}^3/I_{sp}{}^2$ of curve (d) supported this assertion. This combination may be the partially responsible the synergistic lubricating effects between graphene and MoS_2 dispersed in EBO.

The O1s peak at 532 eV was indexed to hydroxides or sulfates, confirming that there was an adsorbed film containing organics or a tribo-film with sulfates on the worn surfaces. The other O1s peak at 530.3 eV was ascribed to –Fe (III) –O– [43], indicating the existence of Fe_2O_3 due to the tribo-oxidation of the matrix during the frictional process. The $Fe_{2p3/2}$ and $Fe_{2p1/2}$ peaks positioned at binding energies of 710.9 eV and 724.5 eV, respectively, belonged to the Fe2p of Fe_2O_3 groups. The simple Fe^0 peaks at 707eV and 719.7eV were not detected in all four samples confirming a similar tribo-oxide film was formed on the worn surfaces under different conditions. The Cr2p peaks at 576.9 eV and 587.6 eV belonged to the $Cr_{2p3/2}$ and $Cr_{2p1/2}$ of Cr_2O_3, respectively, and peaks at 576.1 eV and 585.9 eV belonged to the $Cr_{2p3/2}$ and $Cr_{2p1/2}$ of CrN, a product of the tribo-reaction between matrix Cr and N-containing components in the EBO. However, the peaks at 574.4 eV and 584.2 eV, belonging to the simple Cr^0, were very weak, indicating the rubbed surfaces were covered by the tribo-film. As shown in Fe2p and Cr2p figures, there were no clear differences of the tribo-oxide films containing Fe_2O_3 and Cr_2O_3 among these four lubricating conditions. The tribo-oxide films were dominated by the tribo-reaction between the matrix of steel specimens and organics in EBO

[22].

No obvious Mo3d and S2p signal peaks were detected when lubricated by EBO or EBO+0.5 wt.% graphene. For the EBO+0.5 wt.% MoS_2 or EBO+0.3 wt.% graphene+0.2 wt.% MoS_2 lubrication, the two dominant Mo3d peaks at 232.6 and 235.8 eV were indexed to –Mo (VI)–O– of MoO_3 [44], which are a product of the tribo-reaction of MoS_2, EBO, and the steel specimens during the frictional process. A small peak at 229.7 eV ascribed to Mo3d of MoS_2 was found when lubricated by EBO+0.3 wt.% graphene+0.2 wt.% MoS_2, whereas at the same position there was no clear signal peaks when lubricated by EBO+0.5 wt.% MoS_2. Moreover, the peak areas of the curve (d) were larger than those of curve (c), which indicated that the introduction of graphene and MoS_2 in the EBO contributed to forming an oxide film of MoS_2 on the frictional interfaces. The two S2p peaks at 169 eV and 161.6 eV belonged to –S(VI)–O– of SO_4^{2-} and –Mo–S(II)– of MoS_2, respectively [45]. The peak areas of the curve (d) were also larger than those of curve (c), which was in agreement with the results given in the Mo3d figure. The peak at 161.6 eV in curve (c) was very weak, indicating that MoS_2 was easily removed or oxidized during the frictional process. That is when only MoS_2 was used as an additives in the EBO. The introduction of graphene enhances the adhesion of the MoS_2 on the surface of the specimens and prevents oxidation. This further supports the synergistic lubricating effect of graphene and MoS_2 dispersed in EBO.

According to the above characterization and analysis, the corresponding lubricating mechanisms are summarized in Fig. 15. The rubbing surfaces generated through adsorption a tribo film when lubricated by EBO without additives, with the corresponding wear pattern belonging to adhesive wear. When lubricated by EBO with 0.5 wt.% graphene, the main friction-reduction and antiwear components were the small (and in some cases distorted) graphene particles , and ploughing was the main form of wear. When lubricated by EBO with 0.5 wt.% MoS_2, the MoS_2 was

the main lubricant deposited on the frictional surfaces. The smaller surface area of the MoS_2 and the evident weakness in adsorption, onto the steel substraight meant that any tribo-flims were easy to remove from the surfaces. When lubricated by EBO with 0.3 wt.% graphene and 0.2 wt.% MoS_2, a thicker tribo film was generated on the surfaces. The mutual influence of graphene and MoS_2 during the frictional process, were the main lubricants on the rubbing surfaces, showing a synergistic lubricating effect.

4. Conclusions

The friction and wear behaviors of steel/steel pairs lubricated with EBO and EBO with graphene or/and MoS_2 as additives, were investigated by using a point contact uni-directional sliding tribometer. The synergistic lubricating effects of graphene and MoS_2 on the steel specimens were observed under different frictional conditions. Several surfaces analysis techniques were employed to analyse the lubricating mechanisms. The experimental results indicated that:

1. Graphene and MoS_2 could be dispersed in EBO stably and combined to formulate a lubricant for steel/steel contact. Both of additives lead to a significant decrease in friction coefficient and wear of the steel specimens with 0.5 wt.% content in EBO under different testing conditions. Generally, the graphene possessed a better antiwear effect, whereas the MoS_2 improved friction reduction.

2. The wear mechanisms of the steel specimens were ascribed as follows:

- EBO,- adhesive wear
- EBO with 0.5 wt.% graphene, - ploughing
- EBO with 0.5 wt.% MoS_2, - ploughing and spalling
- EBO with 0.3 wt.% graphene and 0.2 wt.% MoS_2 – ploughing, but at a much

lower rate than above

3. There was an obvious synergistic lubricating effect between the graphene and MoS_2 dispersed in EBO, with this combination showing better tribological behaviors than all of the other EBO/ additive combinations. That is, using graphene/MoS_2 composites as additives for EBO can provide significant improvements in the lubricating properties of bio-oil. Doing so, has the potential to accelerate and expand the application of bio-energy.

4. Under the experimental conditions, normal load and rotating speed affects strength of the synergy between graphene and MoS_2. The optimal frictional conditions were a load of 300N and rotational speed of 850rpm.

5. The lubricating films on the worn surfaces were composed of the following:

- adsorbed organics from the EBO,
- deposit components of graphene and MoS_2,
- tribo-oxide components including Fe_2O_3 and Cr_2O_3, and
- tribo-reacted components such as sulfates, MoO_3 and CrN.

The synergy between the graphene and MoS_2 dispersed in EBO was driven by the formation of thicker adsorbed tribo films, that contained both graphene and organics. A further reason was that graphene enhanced the durability of the MoS_2 films on the frictional surfaces. The mechanisms for this was the prevention of oxidation of the MoS_2 and from being crushed into much small particles. Conversely, the MoS_2 protected the graphene from being crushed into small, defective platelets.

Acknowledgements:

The authors thank Professor Kunhong Hu from Hefei University for his helpful discussions regarding the experimental work. This project is supported by the National Natural Science

Foundation of China (Grant Nos. 51405124, 51450110436), China Postdoctoral Science Foundation (Grant Nos. 2015T80648, 2014M560505) and the Anhui Provincial Natural Science Foundation (Grant No. 1408085ME82). In the UK, the research was supported by equipment purchased by grant number EP/L017725/1.

References

[1] M. Kalin, J. Kogovšek, M. Remškar, Mechanisms and improvements in the friction and wear behavior using MoS_2 nanotubes as potential oil additives, Wear 280–281 (2012) 36-45.

[2] C. Wang, H. Li, Y. Zhang, Q. Sun, Y. Jia, Effect of strain on atomic-scale friction in layered MoS_2, Tribol. Int. 77 (2014) 211-217.

[3] P. Rabaso, F. Ville, F. Dassenoy, M. Diaby, P. Afanasiev, J. Cavoret, B. Vacher, T. Le Mogne, Boundary lubrication: Influence of the size and structure of inorganic fullerene-like MoS_2 nanoparticles on friction and wear reduction, Wear 320 (2014) 161-178.

[4] M. Marquart, M. Wahl, S. Emrich, G. Zhang, B. Sauer, M. Kopnarski, B. Wetzel, Enhancing the lifetime of MoS_2-lubricated ball bearings, Wear 303 (2013) 169-177.

[5] J. Kogovšek, M. Remškar, A. Mrzel, M. Kalin, Influence of surface roughness and running-in on the lubrication of steel surfaces with oil containing MoS_2 nanotubes in all lubrication regimes, Tribol. Int. 61 (2013) 40-47.

[6] W. Zhang, D. Demydov, M.P. Jahan, K. Mistry, A. Erdemir, A.P. Malshe, Fundamental understanding of the tribological and thermal behavior of Ag–MoS_2 nanoparticle-based multi-component lubricating system, Wear 288 (2012) 9-16.

[7] Z.Y. Xu, Y. Xu, K.H. Hu, Y.F. Xu, X.G. Hu, Formation and tribological properties of hollow sphere-like nano-MoS_2 precipitated in TiO_2 particles, Tribol. Int. 81 (2015) 139-148.

[8] L.-Y. Lin, D.-E. Kim, W.-K. Kim, S.-C. Jun, Friction and wear characteristics of multi-layer graphene films investigated by atomic force microscopy, Surf. Coat. Tech. 205 (2011) 4864-4869.

[9] S.S. Kandanur, M.A. Rafiee, F. Yavari, M. Schrameyer, Z.-Z. Yu, T.A. Blanchet, N. Koratkar, Suppression of wear in graphene polymer composites, Carbon 50 (2012) 3178-3183.

[10] D. Berman, A. Erdemir, A.V. Sumant, Few layer graphene to reduce wear and friction on sliding steel surfaces, Carbon 54 (2013) 454-459.

[11] L. Zhang, J. Pu, L. Wang, Q. Xue, Frictional dependence of graphene and carbon nanotube in diamond-like carbon/ionic liquids hybrid films in vacuum, Carbon 80 (2014) 734-745.

[12] X. Fan, L. Wang, Highly conductive ionic liquids toward high-performance space-lubricating greases, Acs Appl. Mater. Interfaces 6 (2014) 14660-14671.

[13] Z. Huang, W. Han, X. Liu, X. Qi, J. Zhong, Graphene/MoS_2 hybrid structure and its photoresponse property, Ceram. Int. 40 (2014) 11971-11974.

[14] Q. Feng, K. Duan, X. Ye, D. Lu, Y. Du, C. Wang, A novel way for detection of eugenol via poly (diallyldimethylammonium chloride) functionalized graphene-MoS_2 nano-flower fabricated electrochemical sensor, Sensors and Actuators B: Chemical 192 (2014) 1-8.

[15] C. Zhai, M. Zhu, D. Bin, F. Ren, C. Wang, P. Yang, Y. Du, Two dimensional MoS_2/graphene composites as promising supports for Pt electrocatalysts towards methanol oxidation, J. Power Sources 275 (2015) 483-488.

[16] L. Ma, J. Ye, W. Chen, D. Chen, J. Yang Lee, Gemini surfactant assisted hydrothermal synthesis of nanotile-like MoS_2/graphene hybrid with enhanced lithium storage performance, Nano Energy 10 (2014) 144-152.

[17] Y. Xu, X. Zheng, H. Yu, X. Hu, Hydrothermal liquefaction of Chlorella pyrenoidosa for bio-oil production over Ce/HZSM-5, Bioresource Technol. 156 (2014) 1-5.

[18] S.W. Kim, B.S. Koo, D.H. Lee, A comparative study of bio-oils from pyrolysis of microalgae and oil seed waste in a fluidized bed, Bioresource Technol. 162 (2014) 96-102.

[19] J.-Y. Kim, S. Oh, H. Hwang, Y.-H. Moon, J.W. Choi, Assessment of miscanthus biomass (Miscanthus sacchariflorus) for conversion and utilization of bio-oil by fluidized bed type fast pyrolysis, Energy 76 (2014) 284–291.

[20] R.N. Hilten, B.P. Bibens, J.R. Kastner, K.C. Das, In-Line Esterification of Pyrolysis Vapor with Ethanol Improves Bio-oil Quality, Energ. Fuel 24 (2010) 673-682.

[21] Y.F. Xu, X.J. Zheng, Y.G. Yin, J. Huang, X.G. Hu, Comparison and Analysis of the Influence of Test Conditions on the Tribological Properties of Emulsified Bio-Oil, Tribol. Lett. 55 (2014) 543-552.

[22] Y. Xu, X. Zheng, X. Hu, K.D. Dearn, H. Xu, Effect of catalytic esterification on the friction and wear performance of bio-oil, Wear 311 (2014) 93-100.

[23] Y. Xu, X. Hu, K. Yuan, G. Zhu, W. Wang, Friction and wear behaviors of catalytic methylesterified bio-oil, Tribol. Int. 71 (2014) 168-174.

[24] Y.F. Xu, H.Q. Yu, X.Y. Wei, Z. Cui, X.G. Hu, T. Xue, D.Y. Zhang, Friction and wear behaviors of a cylinder liner-piston ring with emulsified bio-oil as fuel, Tribol. T. 56 (2013) 359-365.

[25] G. Wang, J. Yang, J. Park, X. Gou, B. Wang, H. Liu, J. Yao, Facile synthesis and characterization of graphene nanosheets, J. Phys. Chem. C 112 (2008) 8192-8195.

[26] T. Kano, Y. Yoshihashi, E. Yonemochi, K. Terada, Clarifying the mechanism of aggregation of particles in high-shear granulation based on their surface properties by using micro-spectroscopy, Int. J. Pharm. 461 (2014) 495-504.

[27] Y. Zhu, Y. Lyu, U. Olofsson, Mapping the friction between railway wheels and rails focusing on environmental conditions, Wear 324–325 (2015) 122-128.

[28] E.E. Nunez, A.A. Polycarpou, The effect of surface roughness on the transfer of polymer films under unlubricated testing conditions, Wear 326–327 (2015) 74-83.

[29] W. Yue, C. Liu, Z. Fu, C. Wang, H. Huang, J. Liu, Synergistic effects between sulfurized W-DLC coating and MoDTC lubricating additive for improvement of tribological performance, Tribol. Int. 62 (2013) 117-123.

[30] K. Zhang, Effects of test conditions on the tribological behaviour of a journal bearing in molten zinc, Wear 259 (2005) 1248-1253.

[31] B.K. Prasad, Sliding wear behaviour of bronzes under varying material composition, microstructure and test conditions, Wear 257 (2004) 110-123.

[32] K.-S. Kim, H.-J. Lee, C. Lee, S.-K. Lee, H. Jang, J.-H. Ahn, J.-H. Kim, H.-J. Lee, Chemical vapor deposition-grown graphene: the thinnest solid lubricant, ACS Nano 5 (2011) 5107-5114.

[33] B.K. Prasad, S. Rathod, M.S. Yadav, O.P. Modi, Sliding wear behavior of cast iron: influence of MoS_2 and graphite addition to the oil lubricant, J. Mater. Eng. Perform. 20 (2011) 445-455.

[34] C. Brecher, S. Bäumler, J. Rossaint, Calculation of kinematics and friction of a spindle bearing using a local EHL friction model, Tribol. T. 56 (2012) 245-254.

[35] G. Chassaing, L. Faure, S. Philippon, M. Coulibaly, A. Tidu, P. Chevrier, J. Meriaux, Adhesive wear of a Ti6Al4V tribopair for a fast friction contact, Wear 320 (2014) 25-33.

[36] M. Varenberg, Towards a unified classification of wear, Friction 1 (2013) 333-340.

[37] Q. Niu, X. Zheng, M. Chen, W. Ming, Study on the tribological properties of titanium alloys sliding against WC-Co during the dry friction, Ind. Lubr. Tribol. 66 (2014) 202-208.

[38] T. Bin, Z. Xiaodong, H. Naisai, H. Jiawen, Study on the structure and tribological properties of CrN coating by IBED, Surface and Coatings Technology 131 (2000) 391-394.

[39] S. Wang, B. Teng, S. Zhang, Torsional wear behavior of monomer casting nylon composites

reinforced with gf: effect of content of glass fiber, Tribol. T. 56 (2013) 178-186.

[40] Y. Xu, X. Zheng, X. Hu, Y. Yin, T. Lei, Preparation of the electroless Ni–P and Ni–Cu–P coatings on engine cylinder and their tribological behaviors under bio-oil lubricated conditions, Surf. Coat. Tech. 258 (2014) 790-796.

[41] B. Román-Manso, E. Domingues, F.M. Figueiredo, M. Belmonte, P. Miranzo, Enhanced electrical conductivity of silicon carbide ceramics by addition of graphene nanoplatelets, J. Eur. Ceram. Soc. 35 (2015) 2723-2731.

[42] G.W. Li, C.S. Li, H. Tang, K.S. Cao, J.A. Chen, F.F. Wang, Y. Jin, Synthesis and characterization of hollow MoS_2 microspheres grown from MoO3 precursors, J. Alloy. Compd. 501 (2010) 275-281.

[43] K. Hu, X. Hu, Y. Xu, F. Huang, J. Liu, The Effect of morphology on the tribological properties of MoS_2 in liquid paraffin, Tribol. Lett. 40 (2010) 155-165.

[44] K.H. Hu, J. Wang, S. Schraube, Y.F. Xu, X.G. Hu, R. Stengler, Tribological properties of MoS_2 nano-balls as filler in polyoxymethylene-based composite layer of three-layer self-lubrication bearing materials, Wear 266 (2009) 1198-1207.

[45] M. JF, W. Stickle, S. PE, B. KD, Handbook of X-ray photoelectron spectroscopy, Phys. Electronics Inc, Eden Prairie, 1995.

Figure Captions

Fig. 1 Particle size distribution of (a) Graphene, (b) MoS_2 , and (c) 0.3 wt. % graphene+ 0.2wt. % MoS_2

Fig. 2 Schematic of the tribological tests

Fig. 3 TEM images and SAED patterns of (a) Graphene and (b) MoS_2

Fig. 4 XRD patterns of (a) Graphene and (b) MoS_2

Fig. 5 (a) Average friction coefficient and (b) WSD and WSW of graphene and MoS_2 dispersed in esterified bio-oil with different mass ratio (Load:300N; Rotating speed: 1000rpm; Additive content: 0.5 wt.%; Testing time: 30min)

Fig. 6 Optical micrographs of the worn surfaces (×100) of the rotating specimens with different test lubricants (graphene and MoS_2 dispersed in liquid paraffin with different mass ratio and total contents of 0.5 wt.%) (a) 0:0, (b) 0:1, (c) 1:4, (d) 2:3, (e) 1:1, (f) 3:2, (g) 4:1, (h) 1:0

Fig. 7 Surface roughness of the worn specimen surfaces under different lubricated conditions

Fig. 8 Effects of loads on (a) Average friction coefficient and (b) WSD and WSW of steel specimens lubricated by EBO with and without additives (Rotational speed: 1000rpm; Testing time: 30min)

Fig. 9 Effects of rotational speeds on (a) Average friction coefficient, (b) WSD, and (c) WSW of steel specimens lubricated by EBO with and without additives (Load:300N; Testing time: 30min)

Fig. 10 SEM images of the worn surfaces of steel/steel pairs lubricated by (a) EBO, (b) EBO+0.5 wt.% graphene, (c) EBO+0.5 wt.% MoS_2, (d) EBO+0.3 wt.% graphene+0.2 wt.% MoS_2

Fig. 11 Particle size distribution of (a) Graphene, (b) MoS_2 and (c) 0.3 wt.% graphene+0.2 wt.% MoS_2 after friction

Fig. 12 Raman spectra of (a) Graphene, (b) MoS_2 and (c) 0.3 wt.% graphene+0.2 wt.% MoS_2

Fig. 13 Illustration of the frictional process of (a) Graphene, (b) MoS_2 and (c) 0.3 wt.% graphene+0.2 wt.% MoS_2

Fig. 14 XPS spectra of the worn surfaces on the rotating specimen lubricated by (a) EBO, (b) EBO+0.5 wt.% graphene, (c) EBO+0.5 wt.% MoS_2, (d) EBO+0.3 wt.% graphene+0.2 wt.% MoS_2

Fig. 15 Schematic explanation of the lubricating mechanisms of (a) EBO, (b) EBO+0.5 wt.% graphene, (c) EBO+0.5 wt.% MoS_2, (d) EBO+0.3 wt.% graphene+0.2 wt.% MoS_2

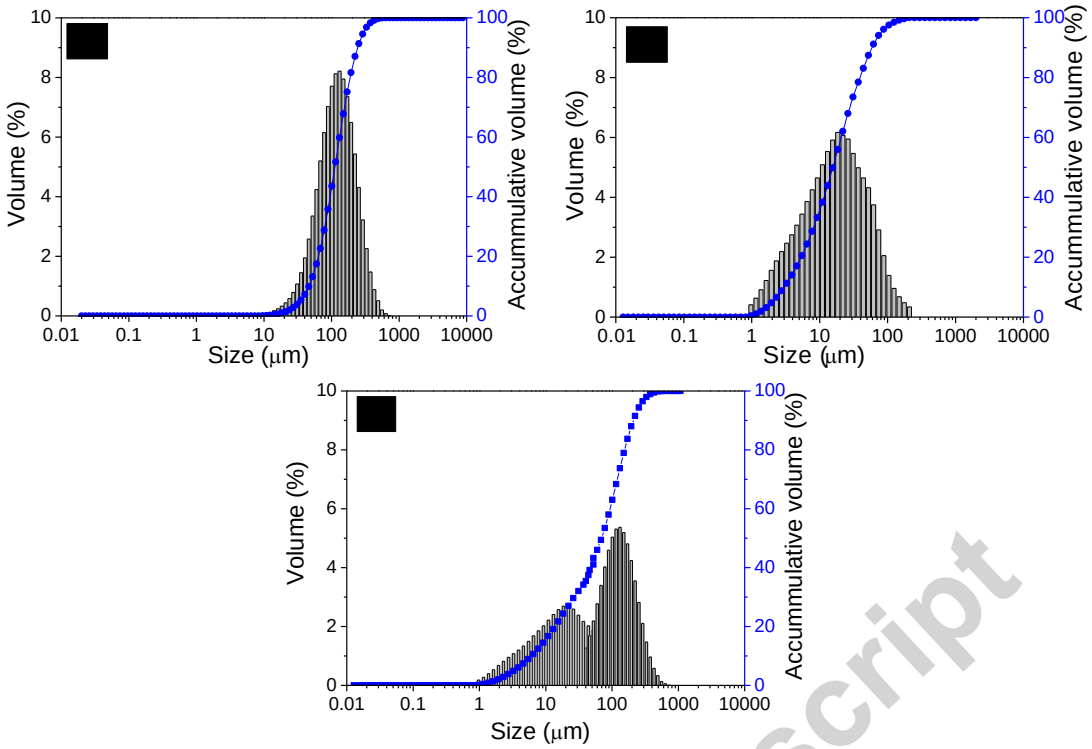

Fig.1 Particle size distribution of (a) Graphene, (b) MoS_2 , and (c) 0.3 wt. % graphene+ 0.2wt. % MoS_2

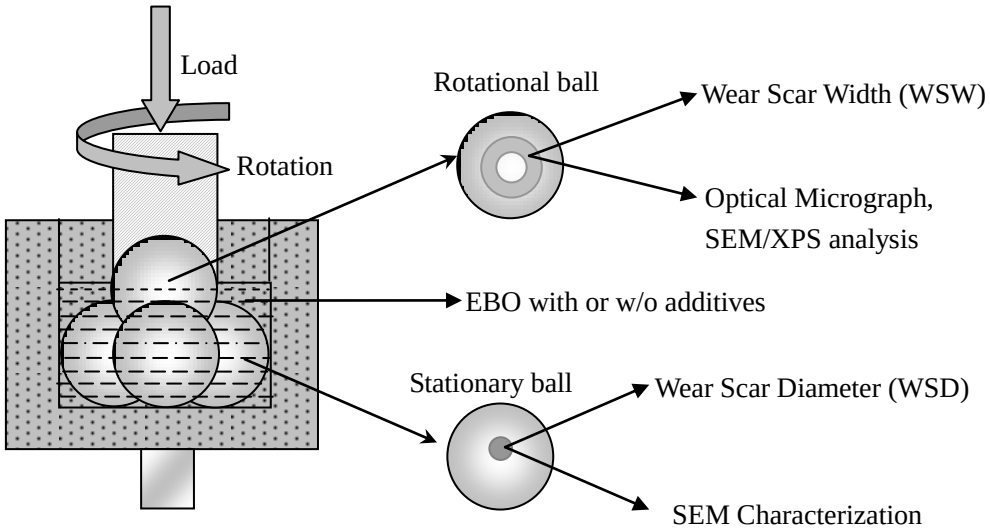

Fig. 2 Schematic of the tribological tests

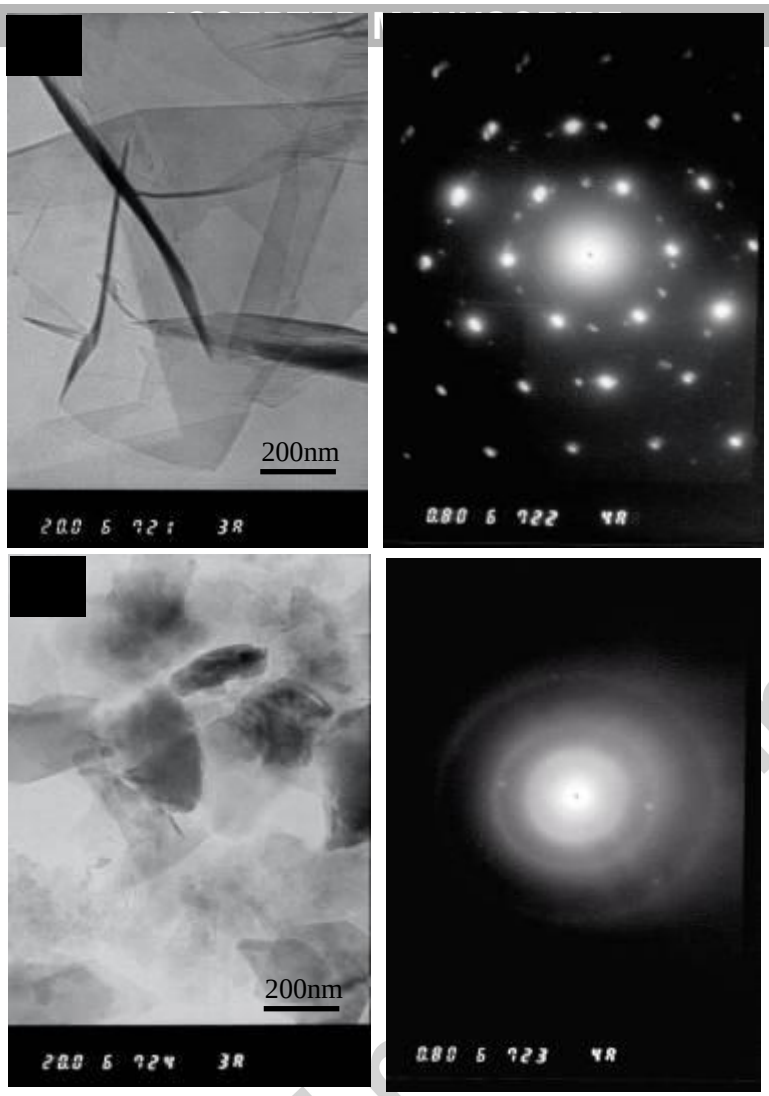

Fig. 3 TEM images and SAED patterns of (a) Graphene and (b) MoS_2

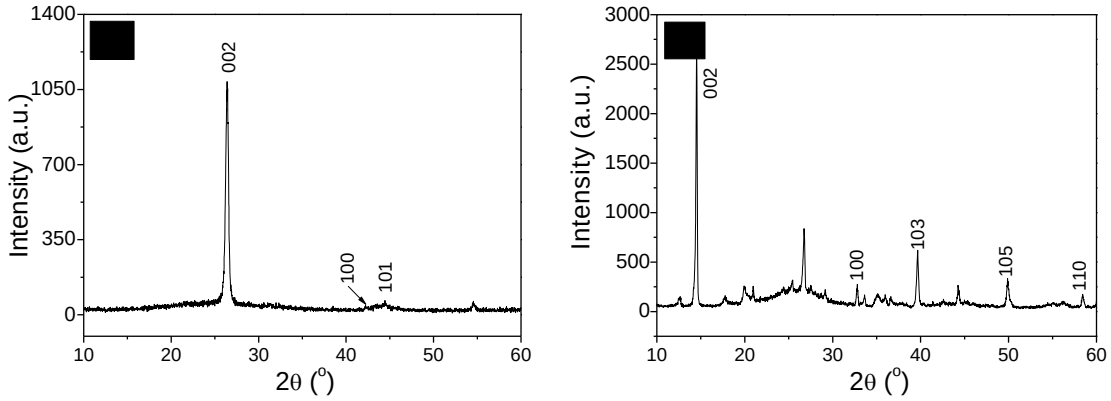

Fig. 4 XRD patterns of (a) Graphene and (b) MoS_2

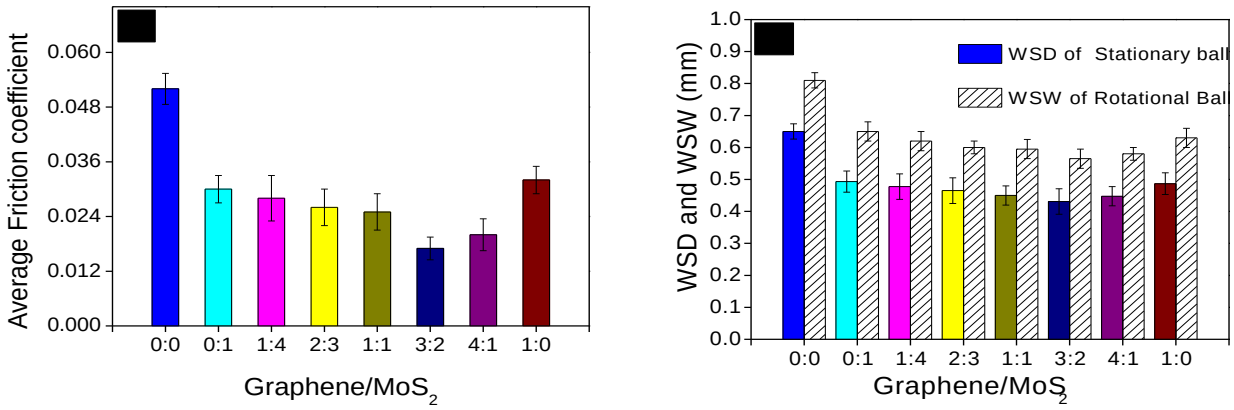

Fig. 5 (a) Average friction coefficient and (b) WSD and WSW of graphene and MoS_2 dispersed in esterified bio-oil with different mass ratio (Load:300N; Rotating speed: 1000rpm; Addtive content: 0.5 wt.%; Testing time: 30min)

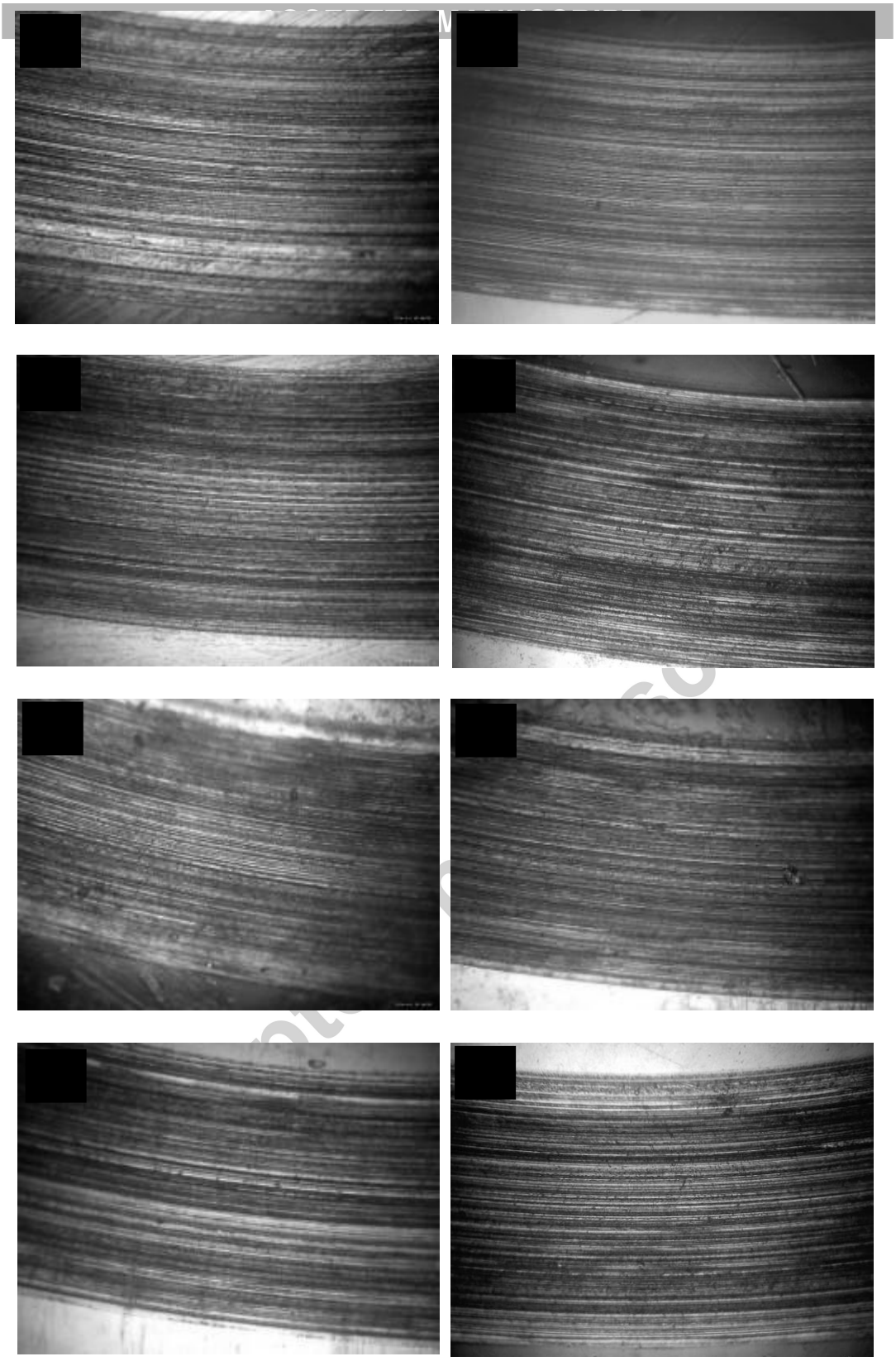

Fig. 6 Optical micrographs of the worn surfaces (×100) of the rotating specimens with different test lubricants (graphene and MoS_2 dispersed in liquid paraffin with different mass ratio and total contents of 0.5 wt.%) (a) 0:0, (b) 0:1, (c) 1:4, (d) 2:3, (e) 1:1, (f) 3:2, (g) 4:1, (h) 1:0

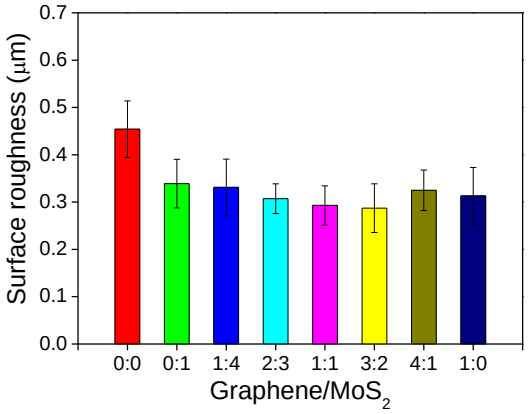

Fig. 7 Surface roughness of the worn specimen surfaces under different lubricated conditions

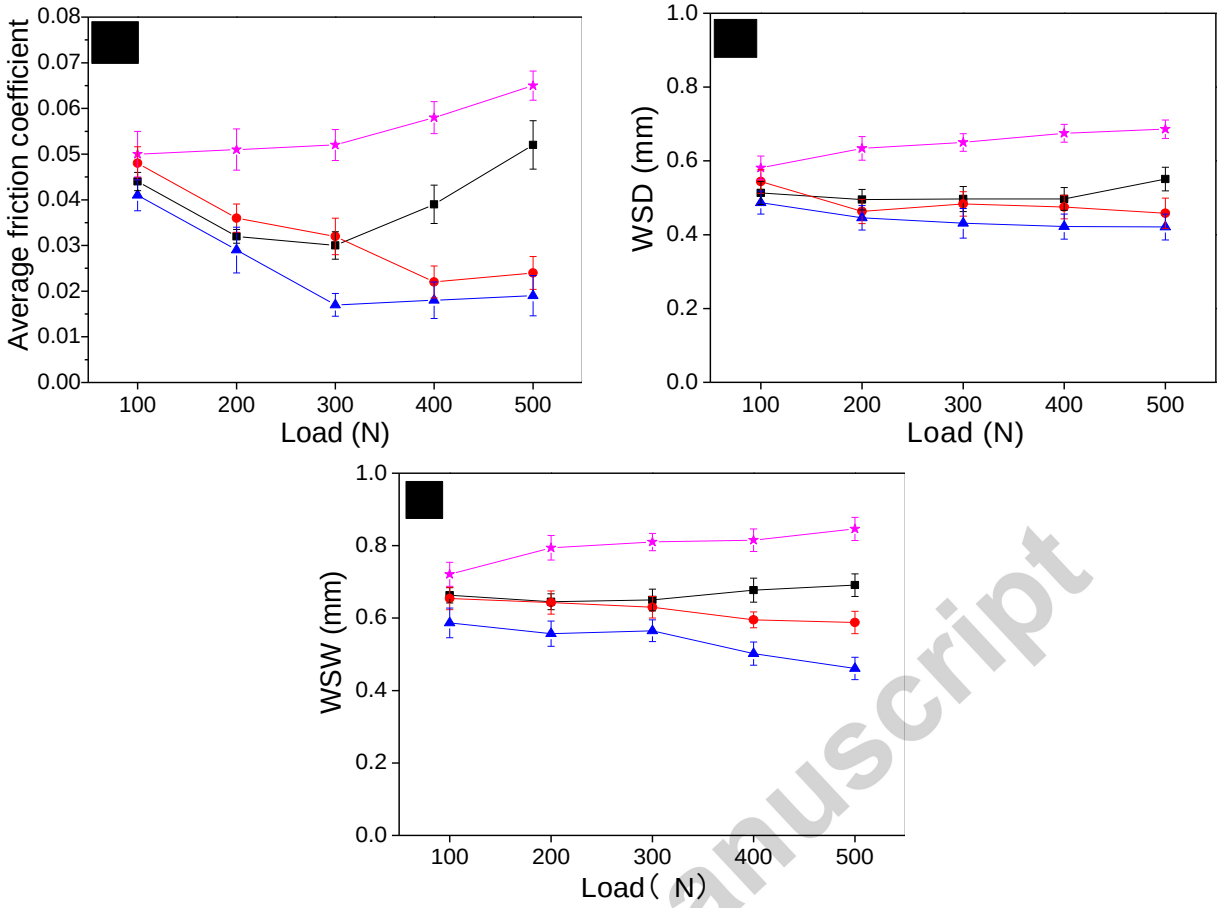

notes: ★ EBO; ● EBO+0.5 wt.% graphene; ■ EBO+0.5 wt.% MoS_2; ▲ EBO+0.3 wt.% graphene+0.2 wt.% MoS_2

Fig. 8 Effects of loads on (a) Average friction coefficient and (b) WSD and WSW of steel specimens lubricated by EBO with and without additives (Rotational speed: 1000rpm; Testing time: 30min)

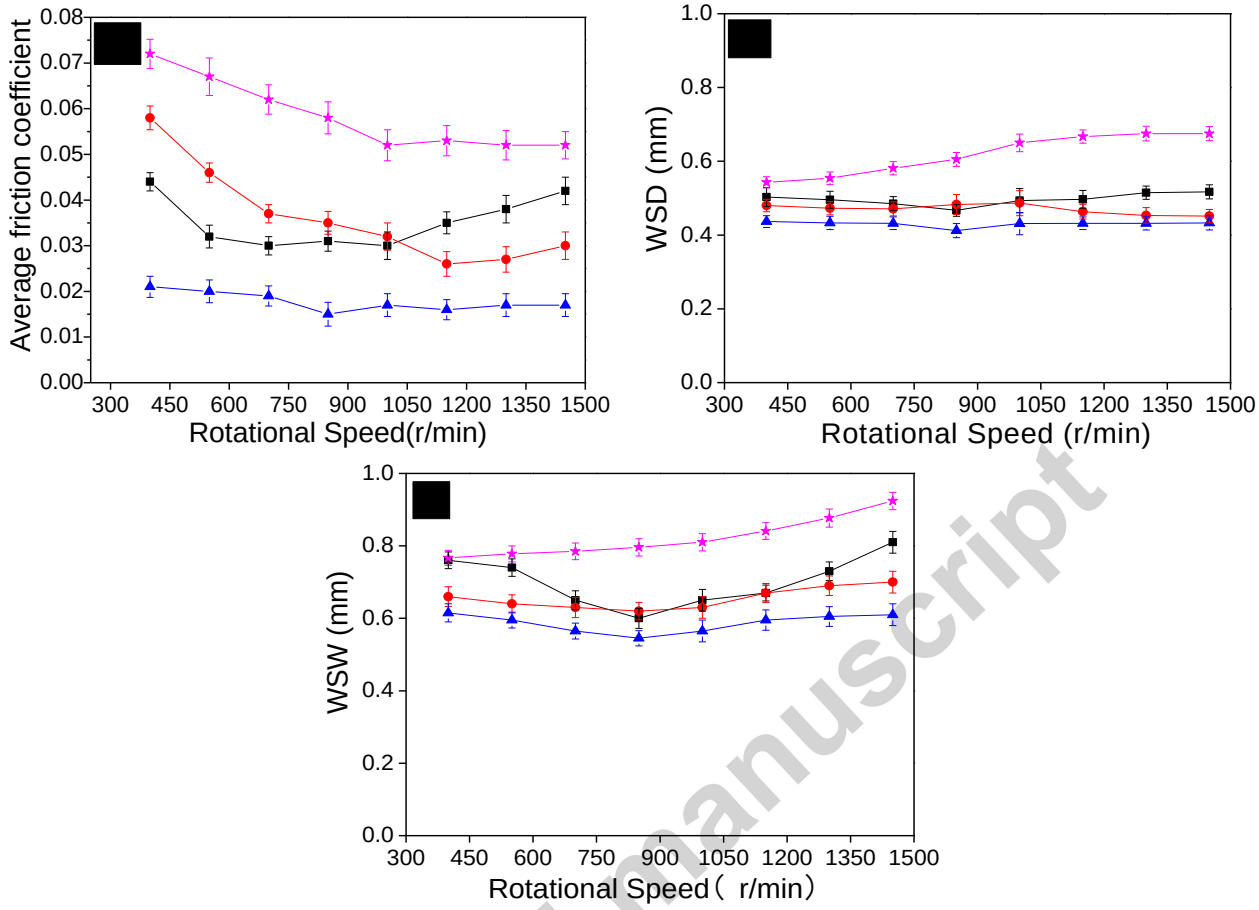

notes: ★ EBO; ● EBO+0.5 wt.% graphene; ■ EBO+0.5 wt.% MoS_2; ▲ EBO+0.3 wt.% graphene+0.2 wt.% MoS_2

Fig. 9 Effects of rotational speeds on (a) Average friction coefficient, (b) WSD, and (c) WSW of steel specimens lubricated by EBO with and without additives (Load:300N; Testing time: 30min)

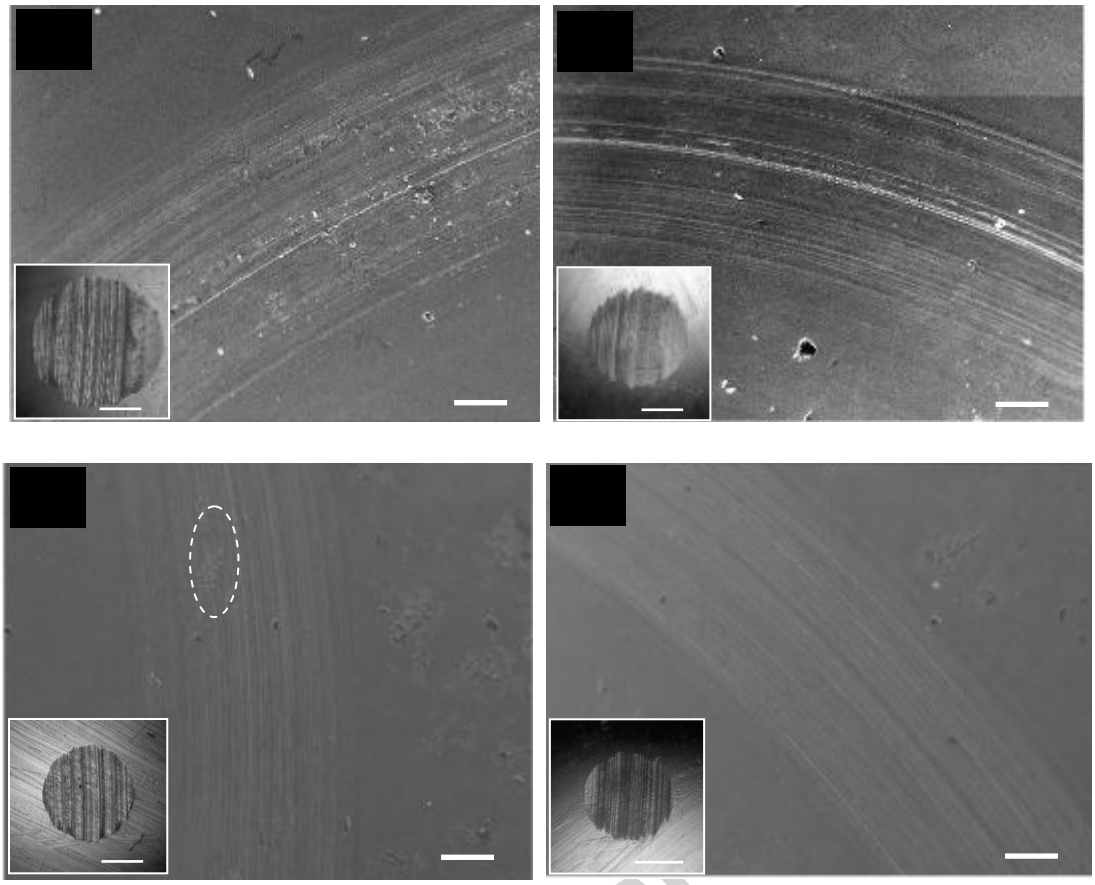

Fig. 10 SEM images of the worn surfaces of steel/steel pairs lubricated by (a) EBO, (b) EBO+0.5 wt.% graphene, (c) EBO+0.5 wt.% MoS_2, (d) EBO+0.3 wt.% graphene+0.2 wt.% MoS_2 (Load:300N; Rotating speed:850rpm; Testing time: 30min)

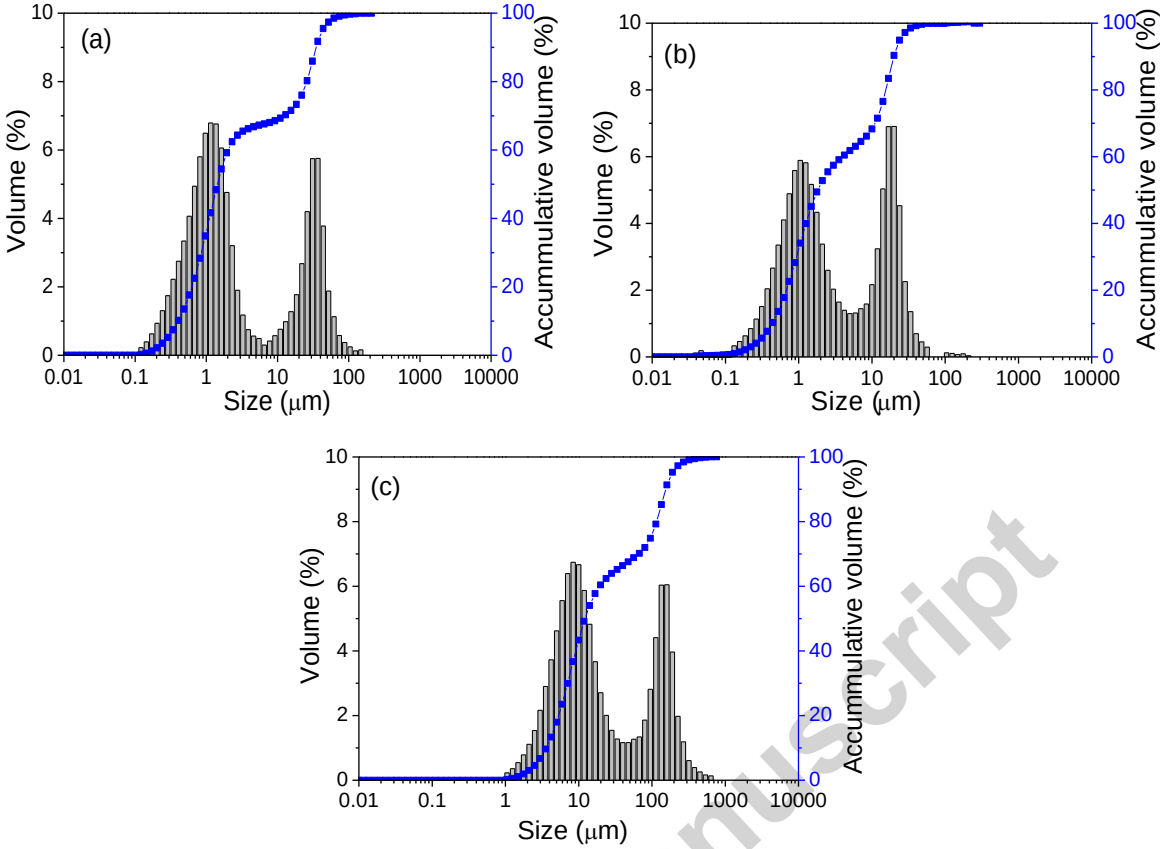

Fig. 11 Particle size distribution of (a)Graphene, (b) MoS_2 and (c) 0.3 wt.% graphene+0.2 wt.% MoS_2 after friction (Load:300N; Rotating speed:850rpm; Testing time: 30min)

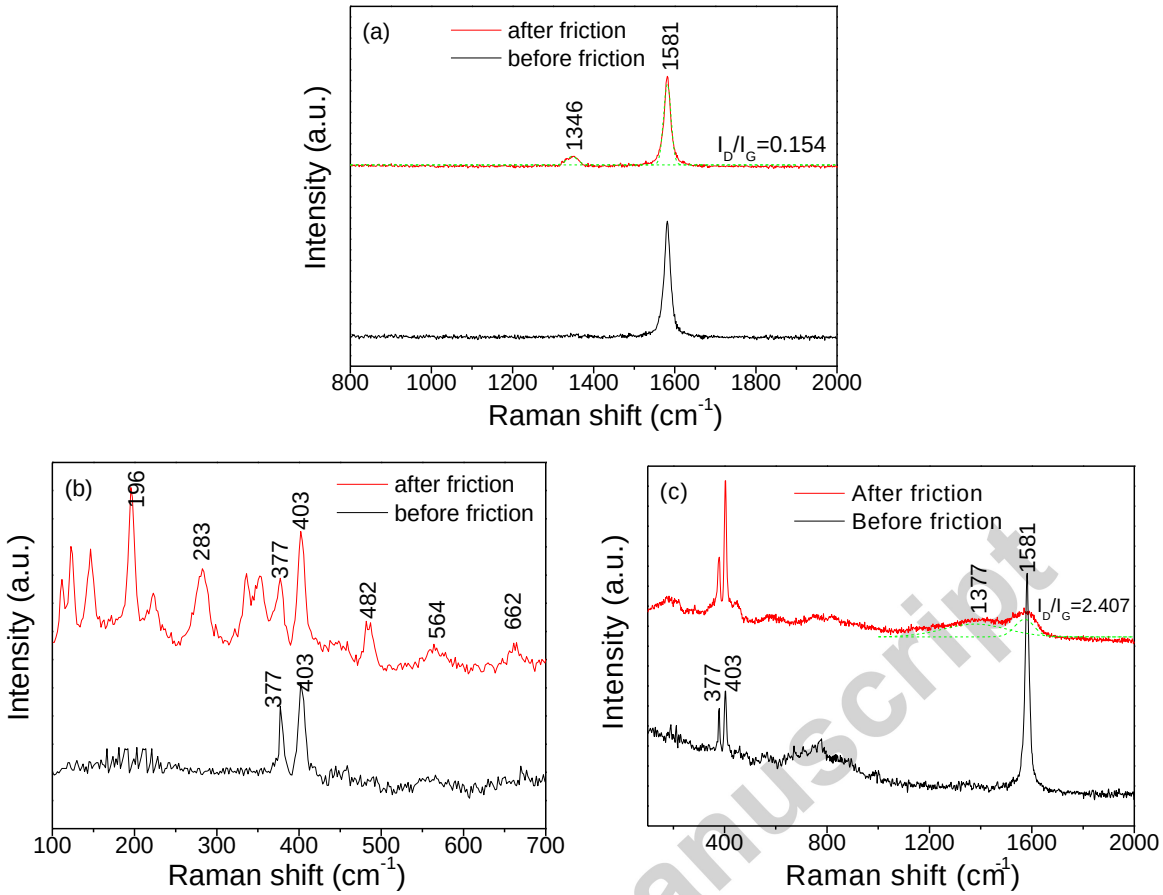

Fig. 12 Raman spectra of (a)Graphene, (b) MoS_2 and (c) 0.3 wt.% graphene+0.2 wt.% MoS_2 before and after friction (Load:300N; Rotating speed:850rpm; Testing time: 30min)

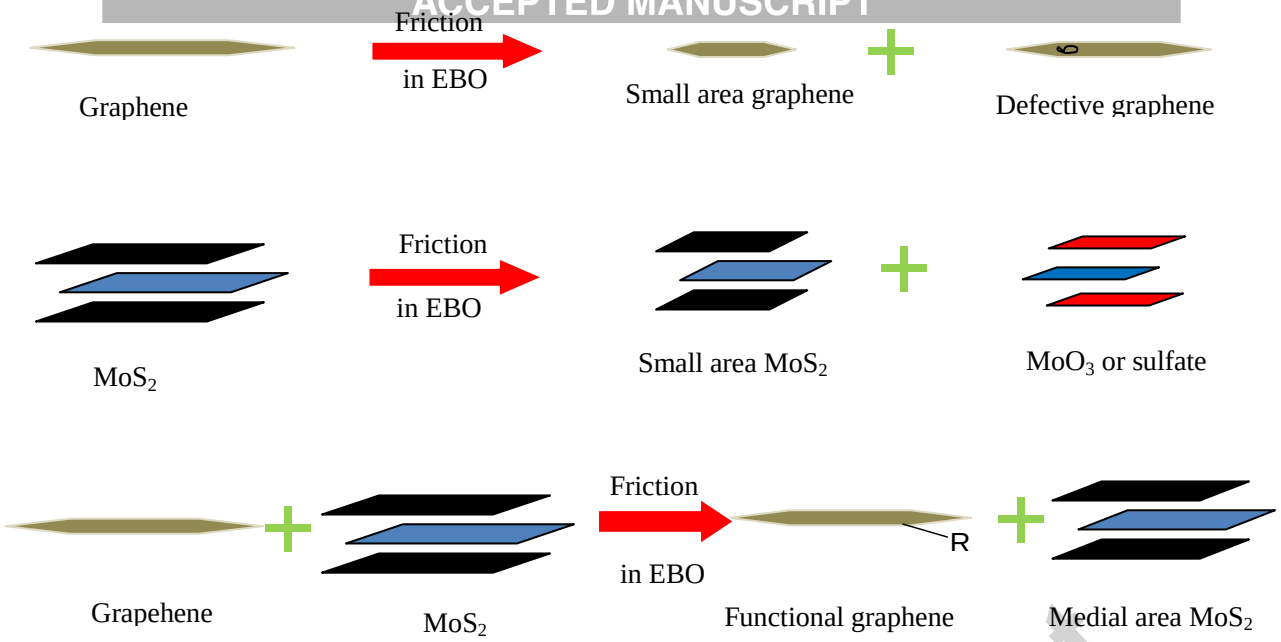

Fig. 13 Illustration of the frictional process of (a) Graphene, (b) MoS_2 and (c) 0.3 wt.% graphene+0.2 wt.% MoS_2

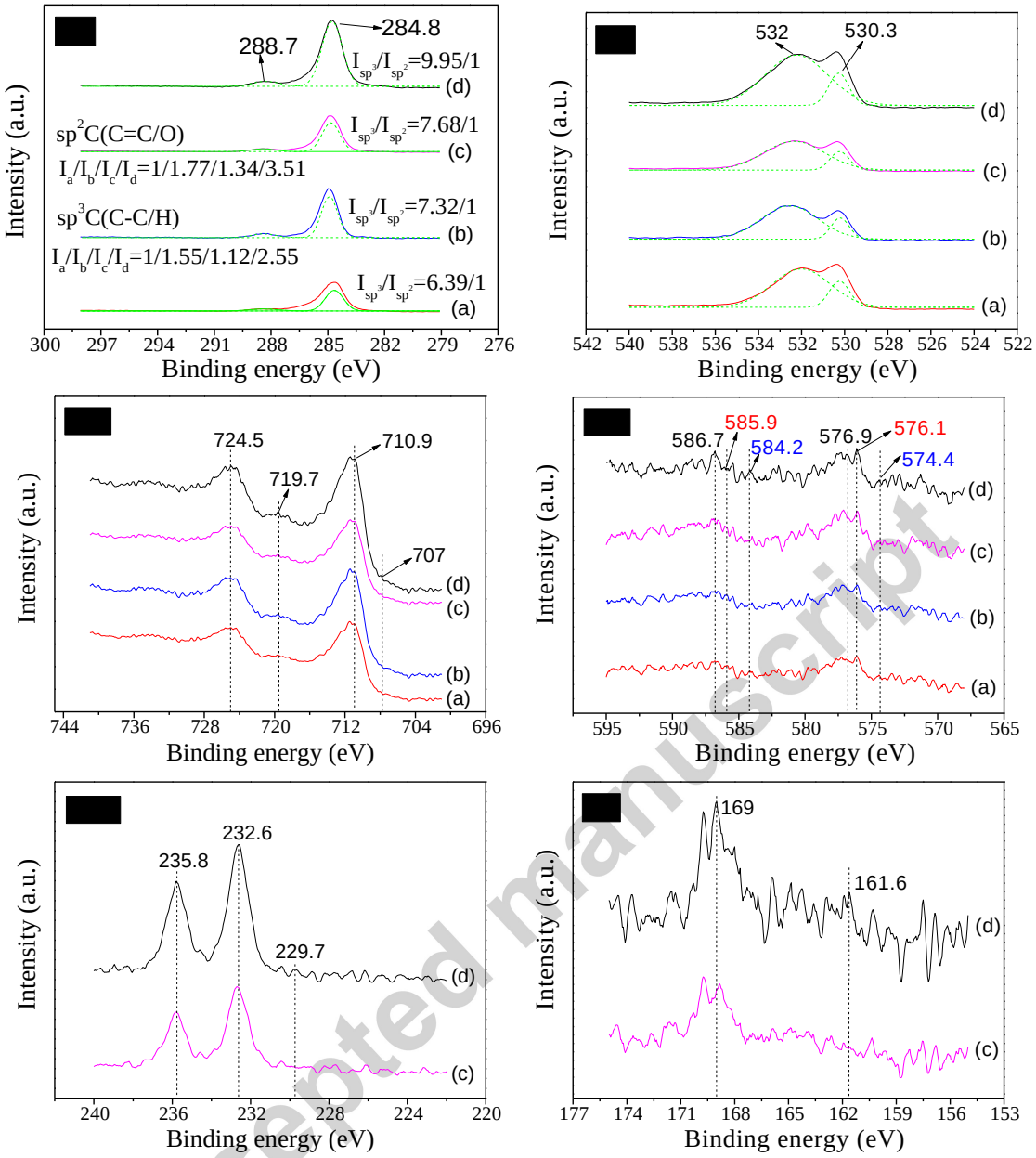

Fig. 14 XPS spectra of the worn surfaces on the rotating specimen lubricated by (a) EBO, (b) EBO+0.5 wt.% graphene, (c) EBO+0.5 wt.% MoS_2, (d) EBO+0.3 wt.% graphene+0.2 wt.% MoS_2 (Load:300N; Rotating speed:850rpm; Testing time: 30min)

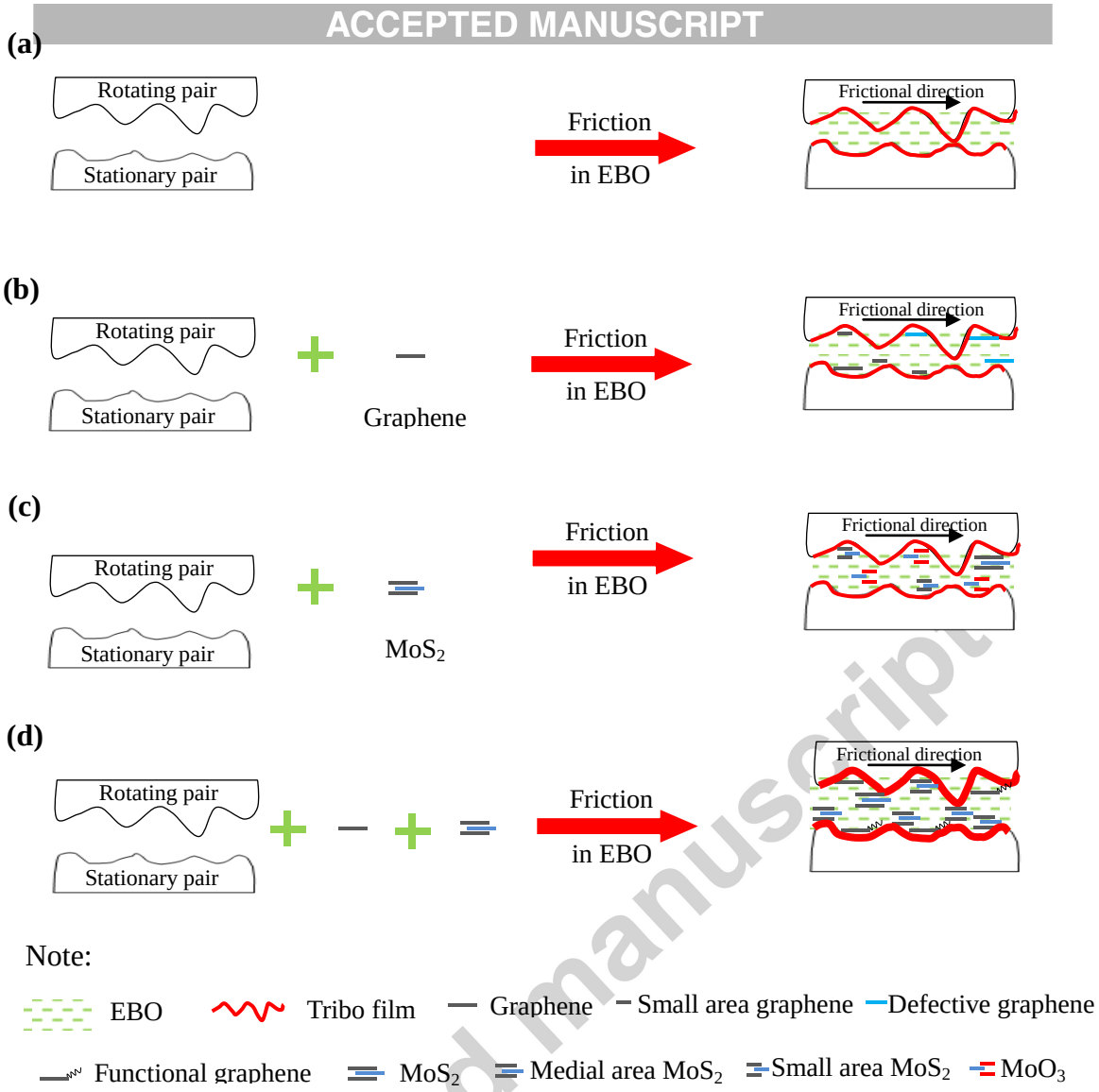

Fig. 15. Schematic explanation of the lubricating mechanisms of (a) EBO, (b) EBO+0.5 wt.% graphene, (c) EBO+0.5 wt.% MoS_2, (d) EBO+0.3 wt.% graphene+0.2 wt.% MoS_2

Highlights:

- Synergistic lubricating roles between graphene and MoS_2 were found.
- Graphene/MoS_2 composites improve the tribological properties of esterified bio-oil.
- Friction and wear behaviors of steel/steel pairs under lubrication were evaluated.
- The corresponding friction and wear mechanism were illuminated.